

Journal Pre-proof

In vitro digestion and bioaccessibility studies of vitamin E-loaded nanohydroxyapatite pickering emulsions and derived fortified foods

Andreia Ribeiro, Raquel F.S. Gonçalves, Ana C. Pinheiro, Yaidelin A. Manrique, Maria Filomena Barreiro, José Carlos B. Lopes, Madalena M. Dias



PII: S0023-6438(21)01859-4

DOI: <https://doi.org/10.1016/j.lwt.2021.112706>

Reference: YFSTL 112706

To appear in: *LWT - Food Science and Technology*

Received Date: 8 July 2021

Revised Date: 15 October 2021

Accepted Date: 24 October 2021

Please cite this article as: Ribeiro, A., Gonçalves, R.F.S., Pinheiro, A.C., Manrique, Y.A., Barreiro, M.F., Lopes, José.Carlos.B., Dias, M.M., *In vitro* digestion and bioaccessibility studies of vitamin E-loaded nanohydroxyapatite pickering emulsions and derived fortified foods, *LWT - Food Science and Technology* (2021), doi: <https://doi.org/10.1016/j.lwt.2021.112706>.

This is a PDF file of an article that has undergone enhancements after acceptance, such as the addition of a cover page and metadata, and formatting for readability, but it is not yet the definitive version of record. This version will undergo additional copyediting, typesetting and review before it is published in its final form, but we are providing this version to give early visibility of the article. Please note that, during the production process, errors may be discovered which could affect the content, and all legal disclaimers that apply to the journal pertain.

© 2021 Published by Elsevier Ltd.

CRedit author statement

Andreia Ribeiro: Methodology, Investigation, Validation; Formal analysis; Writing - Original Draft.

Raquel F. S. Gonçalves: Validation, Writing - Review & Editing.

Ana C. Pinheiro: Methodology, Writing - Review & Editing.

Yaidelin A. Manrique: Methodology, Writing - Review & Editing.

Maria Filomena Barreiro: Conceptualization, Supervision, Writing - Review & Editing.

José Carlos B. Lopes: Conceptualization, Methodology.

Madalena M. Dias: Conceptualization, Supervision, Writing - Review & Editing.

1 ***In vitro* digestion and bioaccessibility studies of vitamin E-loaded**
2 **nanohydroxyapatite Pickering emulsions and derived fortified foods**

3
4
5 Andreia Ribeiro^{1,2}

6 Raquel F. S. Gonçalves³

7 Ana C. Pinheiro³

8 Yaidelin A. Manrique¹

9 Maria Filomena Barreiro^{2,*}

10 José Carlos B. Lopes¹

11 Madalena M. Dias^{1,*}

12
13 ¹Laboratory of Separation and Reaction Engineering – Laboratory of Catalysis and
14 Materials (LSRE-LCM), Faculdade de Engenharia, Universidade do Porto, Rua Dr.
15 Roberto Frias, 4200-465 Porto, Portugal

16 ²Centro de Investigação de Montanha (CIMO), Instituto Politécnico de Bragança,
17 Campus de Santa Apolónia, 5300-253 Bragança, Portugal

18 ³Centre of Biological Engineering (CEB), University of Minho, 4710-057 Braga,
19 Portugal

20
21 * Authors to whom correspondence should be addressed M. F. Barreiro
22 (barreiro@ipb.pt); M. M. Dias (dias@fe.up.pt)

23 **Abstract**

24 Vitamin E is a lipophilic vitamin playing an essential role in human health. Due to
25 oxidative instability, it presents fast degradation and bioactivity loss. In this study,
26 vitamin E-loaded Pickering emulsions stabilized by nano-hydroxyapatite (n-HAp) were
27 produced using a static mixer (NETmix), a technique enabling continuous production and
28 droplet size tailoring. Thus, oil-in-water (O/W) emulsions containing vitamin E at a
29 content of 1mg/mL were produced with different droplet sizes (7.53, 11.56 and 17.72 μm)
30 using an O/W ratio of 20/80 (v/v). Their stability during *in vitro* gastrointestinal digestion
31 and vitamin E bioaccessibility were investigated. It was observed that n-HAp particles
32 disrupt in the stomach and subsequently aggregate as random calcium phosphates in the
33 small intestine, leading to low vitamin E bioaccessibility due to oil entrapment. The
34 emulsion showing the highest vitamin E bioaccessibility ($3.29\pm 0.57\%$, sample with the
35 larger average droplet size) was used to produce fortified gelatine and milk, resulting in
36 an increased bioaccessibility ($10.87\pm 1.04\%$ and $18.07\pm 2.90\%$, respectively). This fact
37 was associated with the presence of macronutrients and the lower n-HAp content. Overall,
38 n-HAp Pickering emulsions offer advantages for vitamin E encapsulation directed to
39 fortified foods development, a process able to be extended to other lipophilic vitamins.

40 *Keywords:* NETmix; Pickering emulsions; Lipophilic vitamin; *in vitro* digestion;
41 Bioaccessibility.

42 **1 Introduction**

43 Vitamin E is a lipophilic vitamin comprising eight compounds, namely: α -, β -, γ - and δ -
44 tocopherol and tocotrienol. Among them, α -tocopherol is the most abundant and
45 biologically active form (Borel, Preveraud, & Desmarchelier, 2013; Burton, 1994; Yang
46 & McClements, 2013). Vitamin E can be naturally found in fresh fruits (kiwi, mango,
47 tomato), vegetables (broccoli, lettuce) and dry fruits (sunflower seeds, hazelnuts, peanuts,
48 almonds) (Borel et al., 2013). Vitamin E intake can avoid cellular ageing and reduce
49 diseases such as dementia, cancer and cardiovascular disorders (Katouzian & Jafari,
50 2016; Niki & Noguchi, 2020; Yang, Decker, Xiao, & McClements, 2015).

51 Vitamin E is currently added to fortified foods, beverages and supplements (Lv, Zhang,
52 Tan, Zhang, & McClements, 2019). However, its effectiveness is not easy to achieve due
53 to its high lipophilic character. Vitamin E cannot be effectively incorporated into aqueous
54 systems and presents oxidative instability, degrading fast and losing bioactivity
55 (Hategekimana & Zhong, 2015; Katouzian & Jafari, 2016). For these reasons, vitamin E
56 is often encapsulated to increase stability, bioavailability, and compatibility with
57 hydrophilic food matrices (Hategekimana, Masamba, Ma, & Zhong, 2015; Lv et al., 2019;
58 Mujica-Álvarez et al., 2020; Yang & McClements, 2013).

59 Among the reported encapsulation systems, Pickering emulsions (PEs), which are
60 emulsifier-free systems, start to be proposed as solutions to increase vitamins
61 bioavailability (Hategekimana et al., 2015; Mitbumrung, Suphantharika, McClements, &
62 Winuprasith, 2019), even some challenges still need to be surpassed. In the work of Lv et
63 al. (2019) dealing with different Pickering stabilizers, vitamin E bioaccessibility was
64 found to be more effective with whey protein systems than with gum Arabic and Quillaja
65 saponin. Comparatively with Tween 80 stabilized emulsions, Zhou et al. (2020) reported
66 a lower vitamin D₃ bioaccessibility using nanochitin PEs, fact associated with the droplet

67 aggregation in the gastrointestinal tract (GIT). Moreover, Winuprasith et al. (2018) who
68 studied vitamin D₃-loaded nanofibrillated cellulose PEs, reported a decreased
69 bioaccessibility rate as the cellulose concentration increased.

70 The reported studies evidence that the bioaccessibility of lipophilic vitamins-loaded PEs
71 depends on several factors. These can be related with the emulsion itself (type of particles,
72 oil phase composition, O/W ratio, and O/W interfacial properties), or with the
73 gastrointestinal environment (presence of calcium ions, bile salts, and phospholipids),
74 which can affect (positively or negatively) the bioaccessibility (Yang et al., 2015).
75 Namely, Zhou et al. (2021) showed that titanium dioxide and nanochitin, when added to
76 milk conjunctly with vitamin D₃, did not significantly affect vitamin bioaccessibility. In
77 another study, Tan et al. (2020) reported that chitosan reduced vitamin D₃ bioaccessibility
78 by binding to the mixed micelles. Summarizing, these results highlight the importance to
79 proceed with the testing of different Pickering systems and their impact on
80 bioaccessibility.

81 In this context, the purpose of the present work was to study vitamin E-loaded n-HAp
82 Pickering emulsions, which were produced using NETmix technology (a static mixer
83 enabling continuous mode), trying to evidence the impact of their droplet size on vitamin
84 E stability, bioaccessibility and bioavailability. HAp is a biocompatible inorganic
85 material mostly used in biomedical and biotechnological applications. This scenario is
86 changing with some food-grade HAp emerging commercially. Thus, following some
87 reported results pointed out Pickering emulsions as promising systems to improve
88 vitamins bioaccessibility, n-HAp stabilized Pickering emulsions were firstly tested as
89 vitamin E carriers, then used to produce fortified milk gelatine and milk. To the best of
90 authors knowledge, this work reports, for the first time, the use of n-HAp Pickering

91 emulsions as vitamin E carriers and the study of emulsion droplet size effect on
92 bioaccessibility.

93 **2 Experimental methods**

94 **2.1 Materials**

95 The *nanoXIM-CarePaste*, hydroxyapatite aqueous paste supplied by Fluidinova S.A., is
96 composed of 15.5 ± 0.5 (wt%) of HAp nanoparticles (n-HAp) with particle size < 50 nm,
97 4.5 ± 0.5 (wt%) KCl and a water content ≤ 81.0 (wt%). This n-HAp has a composition
98 similar to the one commercialized as food grade (*nanoXIM-FoodPaste*). Sunflower oil, a
99 100% vegetable oil obtained from sunflower seeds with a fatty acids composition per
100 100g of 10 g, 28 g and 53 g of saturated, monosaturated and polysaturated, respectively,
101 milk (semi-skimmed) and neutral gelatine (in powder) were purchased from a local
102 supermarket. Other technical properties of the oil include, refractive index of 1.473
103 (determined by refractometry, BOECO Digital, Germany), acid value of 0.72 mg KOH/g,
104 free fatty acids in oleic acid equivalents of 0.36% (Ca 5a-40, according to AOCS (2003)),
105 viscosity of 0.06 Pa·s (determined by rheometry, Anton Paar, GmbH, Austria), and
106 density of 923 kg/m³ (determined by pycnometry). Fluorescent dyes (Nile red - technical
107 grade, and Nile blue A - $\geq 75\%$) and α -tocopherol (98%), further referred as “vitamin E”,
108 were obtained from Sigma-Aldrich. Isopropyl alcohol (99.7%) was purchased from
109 Riedel-de Haen. Pepsin from porcine gastric mucosa (≥ 2500 U·mg⁻¹), bile extract
110 porcine, pancreatin from porcine pancreas (8x USP), Pefabloc® SC and the salts used for
111 the preparation of oral, gastric and intestinal electrolyte solutions were purchased from
112 Sigma-Aldrich. Ethanol (99.8%) and methanol (95%) were purchased from Fisher
113 Scientific, and hexane obtained from VWR Chemicals. Distilled water, treated in a Milli-

114 Q water purification system (TGI Pure Water Systems, Greenville, SC, USA), was used.
115 All other chemicals were of analytical grade.

116 **2.2 Vitamin E-loaded Pickering emulsions production and characterization**

117 Oil-in-water (O/W) PEs were prepared, in continuous mode, according to a previously
118 reported technology, NETmix (Ribeiro, Manrique, Barreiro, Lopes, & Dias, 2021).
119 Briefly, the PEs were obtained using an O/W ratio of 20:80 (v/v). The aqueous phase
120 corresponds to n-HAp (5 wt%) dispersed in water, and the oil phase to a mixture of
121 sunflower oil and vitamin E. Vitamin E was mixed directly in the sunflower oil at a
122 content of 5 mg/mL (oil phase). For each sample 230 mL have been produced.

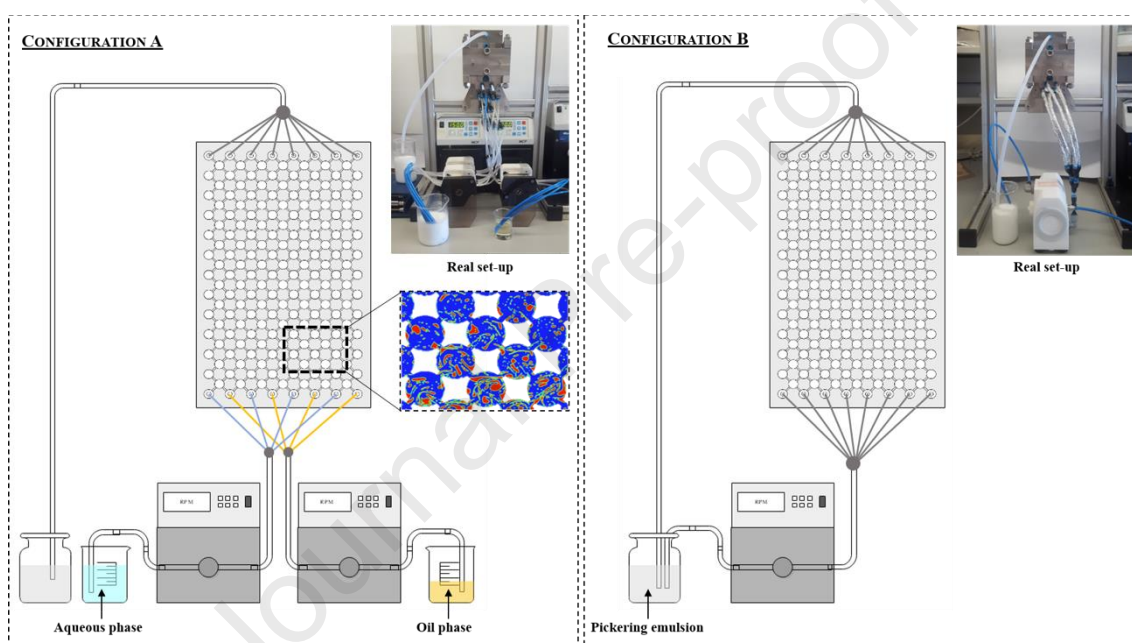
123 NETmix (**Figure 1**) comprises consecutive rows of mixing chambers interlinked by
124 channels, forming a network. The mixing chambers enable successive and well-localized
125 mixing points along the reactor, promoting an easily reproducible emulsification step. To
126 produce the PEs, the NETmix procedure comprised a first step where the aqueous and oil
127 phases are mixed using two peristaltic pumps (Ismatec, Germany) to form a coarse
128 emulsion (pre-emulsion, configuration A). Then, droplet size reduction is achieved by
129 recirculating the pre-emulsion in the NETmix using a diaphragm pump (Almatec,
130 Germany) (configuration B). Recirculation increases the residence time in the NETmix,
131 leading to droplet size reduction. The production conditions in terms of Reynolds number
132 (300 and 400) and the number of cycles (5, 10 and 17) varied according to the required
133 droplet size, as described in **Table 1**. To avoid vitamin E degradation a cooling bath
134 (15 °C, Paar physica viscotherm VT2, The Netherlands) was coupled to the NETmix to
135 control emulsion temperature (18-20 °C). PEs with a proximate droplet size of 7, 11 and
136 18 µm were produced and named as NET-low, NET-middle and NET-high, respectively.
137 The obtained PEs were characterized concerning particle size using a laser diffraction

138 particle size analyser (Beckman Coulter LS230; California) and zeta potential using a
 139 Zetaziser Nano ZS90 (Malvern Instruments, United Kingdom).

140 Table 1: NETmix conditions used to produce the n-HAp stabilized Pickering emulsions.

SAMPLE NAME	Re	CYCLES
NET-low	400	17
NET-middle	400	5
NET-high	300	10

141



142

143 Figure 1: Experimental NETmix set-up used to produce PEs: configuration for the first pass (pre-
 144 emulsion preparation (A), and configuration for the recirculation mode (B).

145 2.3 Vitamin E-fortified foods production

146 To produce the vitamin E-fortified foods, vitamin E-loaded PEs were incorporated in
 147 neutral gelatine and semi-skimmed milk. A ratio of 1:2 of PE to the food matrix was used.
 148 The final concentration of vitamin E in the food matrix was 0.33 mg/mL, higher than the
 149 daily reference intakes of Regulation (EU) no 1169/2011 (1.8 mg or 0.9 mg of vitamin E
 150 per 100 g of food or 100 mL of beverages, respectively). This value was used to facilitate
 151 the quantification of vitamin E by ultra-performance liquid chromatography (UPLC) after
 152 digestion. For the fortified milk, 25 mL of PE were added to 50 mL of milk. The mixture

153 was stirred at 50 rpm for 1 min and stored in the fridge. For the fortified gelatine, 1.5 g
154 of powder gelatine were hydrated with 25 mL of distilled water under stirring, completed
155 with 25 mL at 50 °C (total water 50 mL), then added with 25 mL of the PE. After stirring
156 (50 rpm) for 1 min the final mixture was stored in the fridge to solidify.

157 **2.4 *In vitro* gastrointestinal (GI) digestion studies**

158 The produced vitamin E-loaded PEs (NET-low, NET-middle and NET-high) and fortified
159 foods (milk and gelatine with vitamin E-loaded PEs) were digested *in vitro* to check
160 emulsions' behaviour in case of vitamin E-loaded PEs, and vitamin E bioaccessibility for
161 emulsions and fortified food samples. The harmonized static *in vitro* digestion model
162 described by Minekus et al. (2014) was used. This is a three-stage model comprising the
163 simulation of the mouth, stomach and small intestine conditions. The composition of the
164 simulated digestion fluids is presented in **Table 2**. All fluids and samples (vitamin E-
165 loaded PEs, fortified milk and gelatine) were pre-heated at 37 °C during 5 min.

166 For the oral stage, simulated salivary fluid (SSF), $\text{CaCl}_2(\text{H}_2\text{O})_2$ 0.3 M (to achieve 0.75
167 mM at the final mixture) and Milli-Q water were added to the tested sample (5 mL). The
168 mixture was incubated at 37 °C for 2 min under orbital stirring at 120 rpm. A final ratio
169 of food to SSF of 1:1 (v/v) was targeted. Since the samples did not have starch, α -amylase
170 was not used (Brodkorb et al., 2019). In the gastric stage, simulated gastric fluid (SGF),
171 $\text{CaCl}_2(\text{H}_2\text{O})_2$ 0.3 M (to achieve 0.075 mM at the final mixture) and pepsin solution (with
172 the final activity of 2000 U/mL in the final mixture) were added to the previous mixture.
173 The pH was adjusted to 3.0 with HCl 1 M, and Milli-Q water was added to make up the
174 final volume, and the mixture incubated for 2 h at 37 °C under orbital stirring at 120 rpm.
175 A final ratio of oral sample to SGF of 1:1 (v/v) was targeted. The intestinal stage consisted
176 of simulated intestinal fluid (SIF), $\text{CaCl}_2(\text{H}_2\text{O})_2$ 0.3 M (to achieve 0.3 mM at the final
177 mixture), bile salts (to reach 10 mM at the final mixture) and pancreatin solution (with

178 the final activity of 100 U/mL in the final mixture). The pH was adjusted to 7.0 with
 179 NaOH 1 M or HCl 1 M, then Milli-Q water was added to achieve the final volume. The
 180 samples were incubated for 2 h at 37 °C under orbital stirring at 120 rpm. A final ratio of
 181 gastric sample to SIF of 1:1 (v/v) was targeted.

182 After each stage, samples were collected to check the morphology and stability of vitamin
 183 E-loaded PEs along the simulated gastrointestinal tract. The samples collected at the end
 184 of the gastric stage were maintained in an ice bath to decrease the pepsin activity until
 185 analysis. After complete digestion, the reaction was stopped by adding the enzyme
 186 inhibitor Pefabloc[®] (1 mM) (10 μ L for each 1 mL of the sample). The sample provided
 187 after the intestinal stage was used to analyse bioaccessibility and stability of vitamin E-
 188 loaded PEs and fortified foods. All the samples were tested at least in triplicate.

189

190

Table 2: Composition of simulated digestion fluids.

SALT SOLUTION	SSF (mM)	SGF (mM)	SIF (mM)
KCl	15.1	6.9	6.8
KH ₂ PO ₄	3.7	0.9	0.8
NaHCO ₃	13.6	25	85
NaCl	-	47.2	38.4
MgCl ₂ (H ₂ O) ₆	0.15	0.12	0.33
(NH ₄) ₂ CO ₃	0.06	0.5	-
HCl	1.1	15.6	8.4

191

SSF: simulated salivary fluid; SGF: simulated gastric fluid; SIF: simulated intestinal fluid.

192 2.5 Pickering emulsions digesta characterization

193 Zeta potential can reveal emulsion stability. The emulsion can be considered stable for
 194 high positive (≥ 30) or high negative (≤ -30) values. The determination was done with a
 195 Zetaziser Nano ZS90 (Malvern Instruments, United Kingdom). For that, the PEs were
 196 diluted with distilled water to avoid multiple scattering effects, then placed in a folded

197 capillary Zeta cell (ref: DS7010). The measurement was conducted at 25 °C. Each sample
198 was measured in triplicate and the data expressed as average±standard deviation (SD).
199 To check PEs morphology along digestion, the samples collected at each GIT stage were
200 analysed by CLSM using a Leica TCS-SP5 AOBS (Leica Microsystems, Germany).
201 CLSM is a microscopic technique allowing to observe the particles and oil phase. The
202 digesta sample (100µL) was stained with a mixture of Nile red at 0.1% (w/v) and Nile
203 blue A at 0.1% w/v dissolved in isopropyl alcohol (10µL). Nile blue and Nile red are able
204 to dye the solid particles and the oil phase, respectively. The dyed digesta PE was placed
205 on a slide, and fluorescent dyes excited at 488 nm (Nile red) and at 633 nm (Nile blue A).
206 The images were digitally recorded and processed with a LASX software. The initial PE
207 was also analysed.

208 **2.6 Vitamin E bioaccessibility, stability and bioavailability evaluation**

209 After passing through the three simulated GIT stages, vitamin E concentration was
210 determined according to the procedure described by Lv et al. (2019) with some
211 modifications. Briefly, the digesta obtained after the small intestine stage was centrifuged
212 (Allegra 64R, Beckman Coulter Inc., USA) at 18700 g and 4 °C for 30 min to obtain the
213 micellar phase. Before UPLC (Nexera X2, Shimadzu, Japan) analysis, vitamin E was
214 extracted from digesta and micellar phase samples. For that, 3 mL of the sample were
215 mixed with 3 mL of a hexane/ethanol mixture (1/1, v/v), then centrifuged at 4000 rpm for
216 2 min (Multifuge X3R, Heraeus, Germany) to obtain a supernatant layer. This extraction
217 was repeated three times, and the obtained supernatant layers mixed and dried under
218 nitrogen. The dried samples were dissolved in methanol and filtered through a 0.22 µm
219 filter. The vitamin E concentration was determined using a UPLC with a C18 column
220 (150×2.1 mm, 1.7 µm, Kinetex[®]) using a mixture of 95% methanol and 5% double-
221 distilled water as the mobile phase. An isocratic elution mode at 0.4 mL/min, with a

222 column temperature of 40 °C and a 10 µL injection volume were used. The detection
 223 wavelength for vitamin E was 295 nm.

224 Vitamin bioaccessibility was determined by measuring the concentration of vitamin E in
 225 the mixed micelle ($C_{micelle}$) and digesta phases ($C_{digesta}$) using the following equation:

$$Bioaccessibility = \frac{C_{micelle}}{C_{digesta}} \times 100 \quad (1)$$

226 Stability was calculated as the vitamin E fraction remaining untransformed in the small
 227 intestine and calculated as

$$Stability = \frac{C_{digesta}}{C_{initial}} \times 100 \quad (2)$$

228 where, $C_{initial}$ represents the vitamin E concentration in the initial stage, i.e., the vitamin
 229 E concentration of the PE (1 mg/mL).

230 The bioavailability of the vitamin E was then estimated as the product of bioaccessibility
 231 and stability

$$Bioavailability = Bioaccessibility \times Stability \quad (3)$$

232 The calculated bioavailability corresponds to an estimative of vitamin E absorption.

233 **2.7 Statistical analysis**

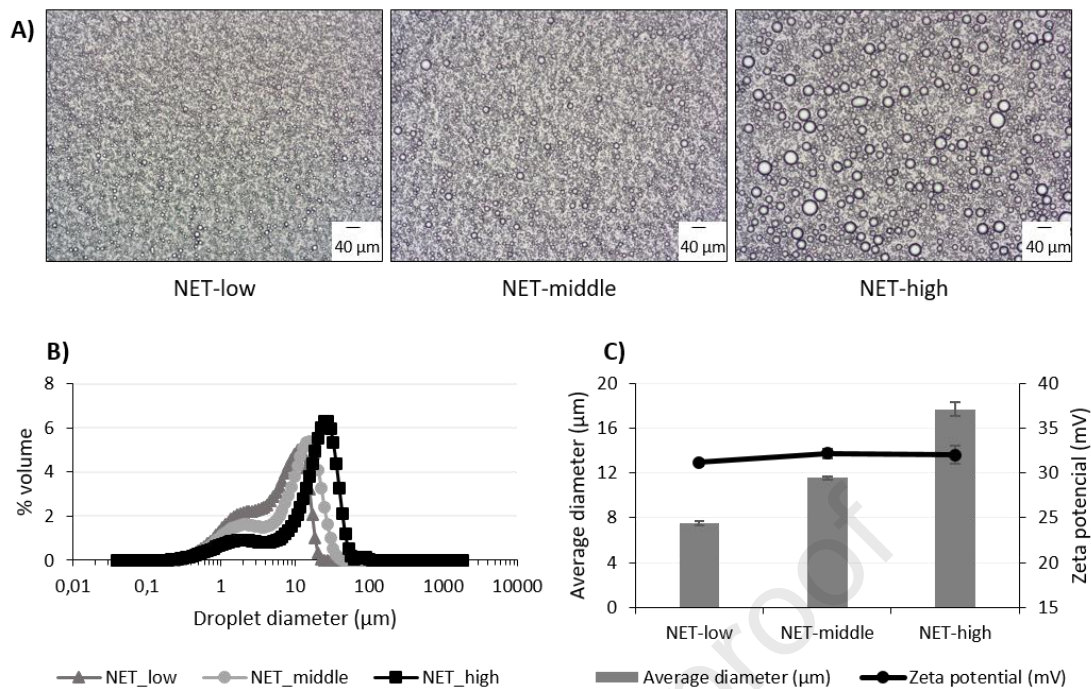
234 The digestion and bioaccessibility studies of PEs and fortified foods were done in
 235 triplicate and duplicate, respectively. Data is presented as average±SD. The statistical
 236 analysis was performed using the commercial software IBM SPSS statistics (version 27.0,
 237 SPSS Inc., Chicago, IL, USA). One-way analysis of variance of independent variables
 238 followed by Tukey's test was carried out on the digesta PEs measurements to establish
 239 significant differences ($p<0.05$). For fortified foods measurements, a t -test was used to
 240 determine the significant difference among the tested samples ($p<0.05$).

241 **3 Results and discussion**

242 **3.1 Vitamin E-loaded Pickering emulsions characterization**

243 The vitamin E-loaded PEs with tailored droplet average sizes were produced using
244 NETmix according to the parameters described in **Table 1**. The influence of these
245 parameters in the average droplet size of the emulsion was previously reported by Ribeiro
246 et al. (2021), and adopted in this study since the used vitamin E concentration did not
247 impacted the sunflower oil viscosity (0.06 Pa·s).

248 **Figure 2** shows the optical microscopy images of NET-low, NET-middle and NET-high
249 samples with the determined droplet size distributions, average droplet size (7.53, 11.56
250 and 17.72 μm , respectively) and zeta potential (+31.18, +32.20, and +32.05 mV,
251 respectively). In terms of the zeta potential, similar values were obtained for the 3
252 samples; namely, the produced PEs were characterized by a strong positive zeta potential,
253 indicating that droplet aggregation is inhibited resulting in stable emulsions due to an
254 electrostatic repulsion mechanism.



255

256 Figure 2: Optical images (A), droplet size distributions (B), average size distributions (μm) and zeta
 257 potential (mV) (C) of the produced vitamin E-loaded Pickering emulsions produced using NETmix
 258 technology.

259 3.2 Vitamin E-loaded Pickering emulsions gastrointestinal digestion

260 The vitamin E-loaded PEs were digested *in vitro* through a simulated GIT. After each
 261 stage (mouth, gastric and intestine phases), a sample was collected for analysis, namely
 262 concerning for microstructure (CLSM), zeta potential, vitamin E bioaccessibility and
 263 stability analysis.

264 3.2.1 Influence on microstructure morphology

265 **Figure 3** shows the CLSM analysis of the studied PEs (NET-low, NET-middle, and NET-
 266 high) in the initial stage and throughout the simulated GIT. The red fluorescence colour
 267 represents n-HAp particles (dyed by Nile blue), whereas the green fluorescence colour
 268 represents the oil phase (stained by Nile red).

269 At the initial stage, a packed n-HAp layer is observed around the oil droplets for all tested
 270 PEs, confirming the efficient stabilization role of the nanoparticles. After exposure to the
 271 mouth stage, the number of oil droplets decreased, justified by the dilution applied in the

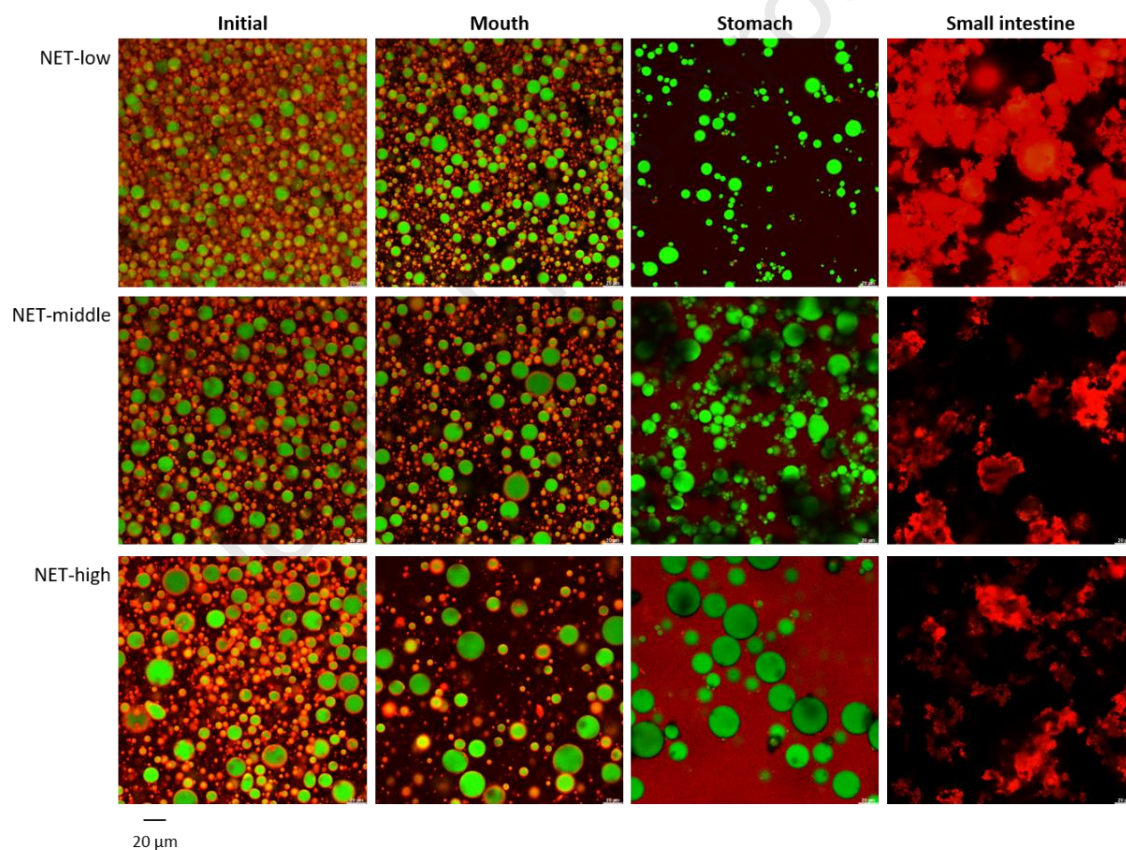
272 digestion model. In this stage, no changes in the n-HAp stabilizing role were perceived,
273 i.e., the n-HAp particles maintained their tight position at the oil surface. Also, for all the
274 tested samples, no evident changes in the droplet size were observed, and no agglomerates
275 were detected.

276 In the stomach, the PEs face stringent conditions, namely they contact with gastric fluids
277 characterized by a highly acidic pH (around 1-3), relatively high ionic strength (around
278 150 mM), and a high enzymes content (McClements, 2016). The acquired CLSM images
279 (**Figure 3**) revealed that this is the first local in GIT where the PEs undergo strong
280 changes. Namely, it is evident that the n-HAp particles are not covering the oil droplets,
281 i.e., they are not acting anymore as Pickering stabilizers in all tested PEs. The n-HAp
282 particles seem to have disrupted, becoming dissolved in the aqueous medium, fact
283 compatible with the observation of a quite uniform red background. In fact, the Nile blue,
284 which dyes the hydrophilic compounds, might be staining the Ca^{2+} and PO_4^{2-} species of
285 the disrupted n-HAp particles, and other molecules resulting from the two digestive
286 stages. These results are in agreement with Ramis, Coelho, Córdoba, Quadros, and Monjo
287 (2018) that studied the n-HAp paste behaviour in simulated gastric fluid, identifying its
288 rapid and complete dissolution under gastric environment after 7.5 min at 37 °C. In this
289 work, together with particle's disruption, a slight oil droplet size increase was observed
290 after exposure to gastric conditions, which may also be justified by the n-HAp detachment
291 from the oil droplets facilitating coalescence.

292 After passing the stomach, medium in which the n-HAp particles become completely
293 dissolved, the digestion proceeds to the small intestine. Within this phase, the
294 environment conditions change, namely the pH turn to neutral. Under these conditions,
295 and as shown in the CLSM images taken after the intestine phase (**Figure 3**), appreciable
296 changes were noticed. The material of the dissolved n-HAp particles coming from the

297 stomach phase forms large and random calcium phosphate clusters upon in contact with
 298 neutral pH. This result corroborates the observations made by Epple (2018) that reported
 299 the precipitation of HAp in random calcium phosphate clusters at neutral pH after
 300 contacting acidic pH.

301 The PEs tailored with different sizes showed similar behaviour during GI digestion with
 302 apparent stability in mouth stage, n-HAp disruption in gastric conditions and aggregates
 303 formation in intestinal conditions. However, NET-low PE has larger aggregates than the
 304 other samples after intestinal phase (**Figure 3**).



305

306 Figure 3: Overlapped CLMS images of the vitamin E loaded Pickering emulsions with different sizes
 307 (NET-low= $\sim 7 \mu\text{m}$, NET-middle: $\sim 11 \mu\text{m}$; NET-high: $\sim 18 \mu\text{m}$) after each stage of digestion (mouth,
 308 stomach and small intestine), comparatively with the initial emulsion. The n-HAp particles and the oil
 309 droplets are presented as red and green colour, respectively. For interpretation of the references to the
 310 colour in this figure legend, the reader is referred to the web version of the article. The images were taken
 311 with a magnification of 20x and zoom of 3x.

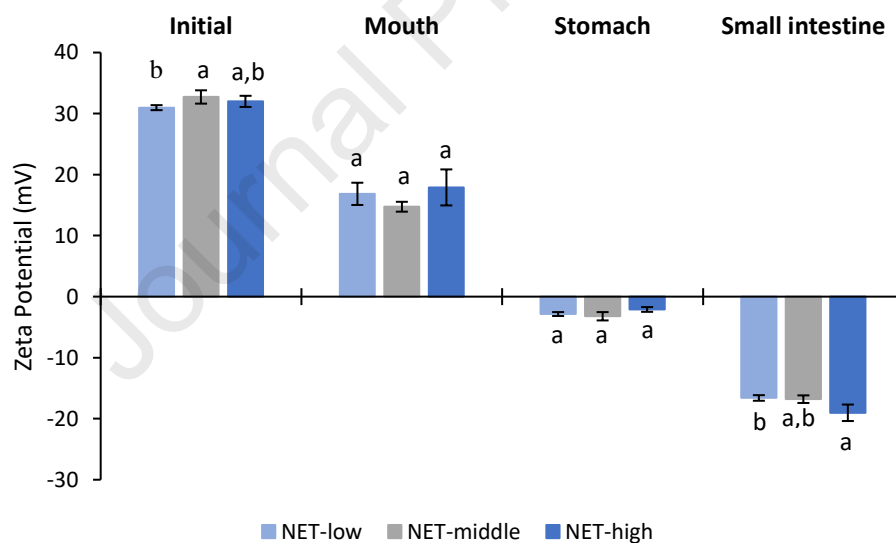
312 3.2.2 Influence on zeta potential

313 **Figure 4** shows the zeta potential of the studied PEs (NET-low, NET-middle, NET-high)
314 throughout the simulated GIT. For comparison purposes, the zeta potential of the initial
315 emulsions is included. The statistical analysis was done for each stage by comparing the
316 zeta potential value of the three tested emulsions with different droplet size. It was
317 observed that the value changes throughout the GIT, including the surface charge shifts
318 from positive to negative between the mouth and stomach. The three emulsions presented
319 similar behaviour for all GIT stages ($p < 0.05$).

320 The contact with the mouth promoted an appreciable decrease in the zeta potential
321 magnitude (from approximately from 32 mV to 16 mV), probably associated with the
322 neutral pH of this stage and the adsorption of ionic species at the droplets' surface. After
323 mouth stage, no statistical differences were observed between the three emulsions
324 ($p < 0.05$) meaning a similar behaviour for the PEs regardless the size. These results
325 suggest that PEs become more prone to instabilities after the mouth stage. In accordance,
326 other authors working with PEs stabilized with nanofibrillated cellulose observed small
327 changes in the droplet size and morphology after this first digestion phase, which was
328 related to mucin presence (Winuprasith et al., 2018).

329 Upon in the stomach, the PEs zeta potential becomes low in magnitude and negative
330 (around -3 mV) and once again no statistical differences were observed between the three
331 emulsions ($p < 0.05$). This change can be attributed to the highly acidic pH of the gastric
332 fluids together with the presence of enzymes (i.e., pepsin), which can lead to the
333 adsorption of negatively charged molecules neutralizing the positive charge (Zhou et al.,
334 2020). Also, the high ionic strength medium can have contributed to the emulsion
335 destabilization. These observations agree with the CLSM images acquired after the
336 stomach stage (**Figure 3**).

337 In the small intestine, all the tested PEs presented a relatively strong negative zeta
 338 potential (but not high enough to be considered stable), which can be attributed to the
 339 presence of bile acids, phospholipids, and free fatty acids generated from the digestion of
 340 the emulsified oil (triglycerides). These molecules are negatively charged, leading to a
 341 zeta potential decrease. This observation is in accordance with the work of Zhou et al.
 342 (2020) that reported a strong zeta potential decrease for emulsions after the small intestine
 343 stage, fact associated with the presence of bile acids and peptides. Comparing the three
 344 emulsions, after small intestine stage there was significant differences ($p<0.05$), namely
 345 between NET-low and NET-high. NET-high had stronger negative zeta potential value,
 346 possibly indicating more effective adherence of the bile acids and others species at the
 347 cluster's surface.



348

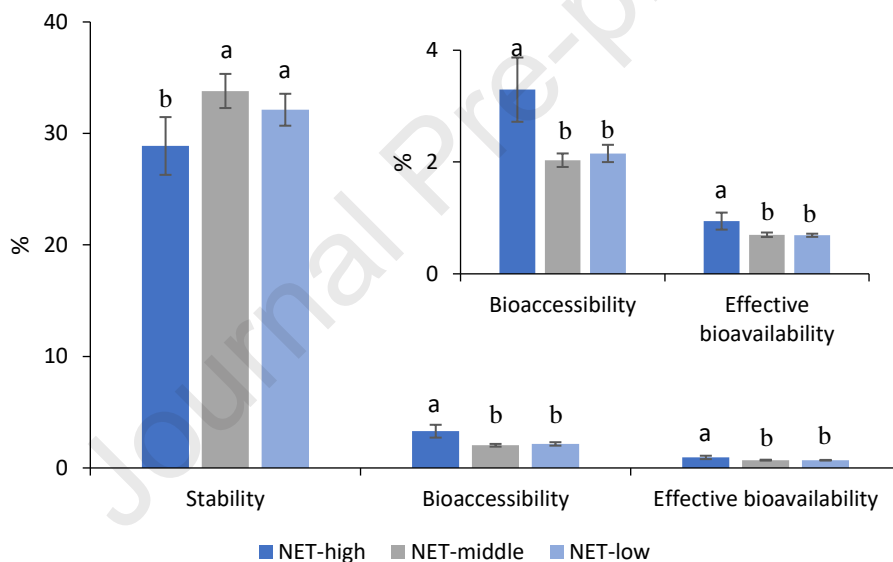
349 Figure 4: Zeta potential of the vitamin E-loaded Pickering emulsions (NET-low= ~7 μm , NET-middle:
 350 ~11 μm ; NET-high: ~18 μm) along the gastrointestinal tract (mouth, stomach and small intestine),
 351 comparatively with the initial emulsion. In each GIT stage, different letters represent significant
 352 differences between the Pickering emulsions ($p<0.05$).

353

354 3.2.3 Influence on vitamin E bioaccessibility and stability

355 In this section, the influence of the GI digestion on vitamin E stability and bioaccessibility
 356 was evaluated (Figure 5), and the statistical analysis was done to compare the three

357 emulsions for each evaluated parameter. In general, all PEs presented a high vitamin E
 358 stability. The NET-high sample showed the lowest and statistically different vitamin E
 359 stability followed by NET-low and NET-middle, respectively, $28.9 \pm 2.59\%$, $32.1 \pm 1.43\%$
 360 and $33.8 \pm 1.53\%$ ($p < 0.05$). However, all emulsions exhibited low vitamin E
 361 bioaccessibility, with NET-high sample presenting a slightly higher and statistically
 362 different value, comparatively with NET-low and NET-middle, respectively,
 363 $3.29 \pm 0.57\%$, $2.15 \pm 0.15\%$ and $2.03 \pm 0.12\%$ ($p < 0.05$). Therefore, NET-high sample
 364 presented the highest value of calculated bioavailability, followed by NET-middle and
 365 NET-low, $0.94 \pm 0.15\%$, $0.70 \pm 0.03\%$ and $0.69 \pm 0.03\%$, respectively ($p < 0.05$).



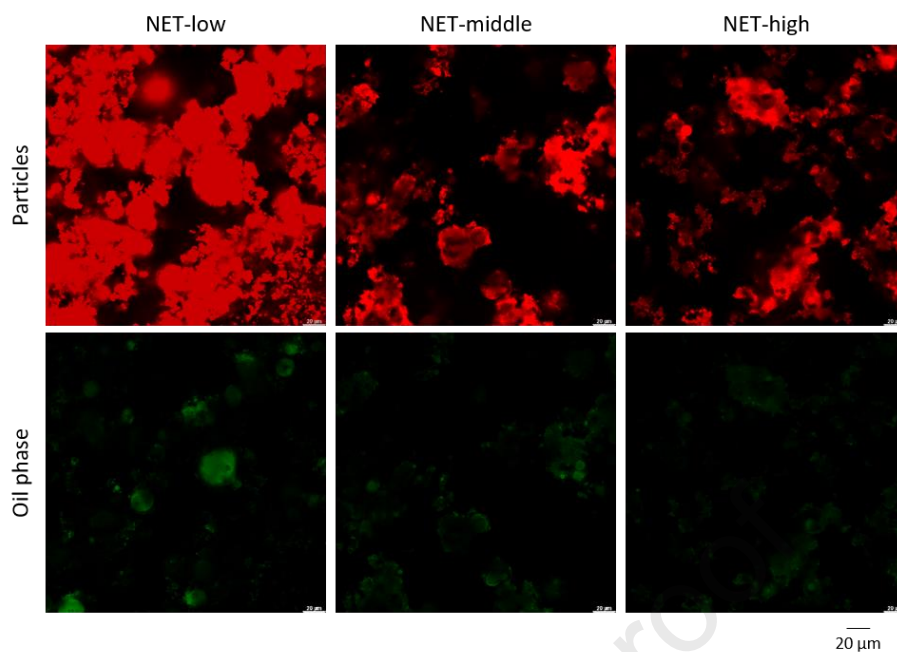
366

367 Figure 5: Bioaccessibility, stability and effective bioavailability of vitamin E loaded Pickering emulsions
 368 with different particle's sizes (NET-low= $\sim 7 \mu\text{m}$, NET-middle: $\sim 11 \mu\text{m}$; NET-high: $\sim 18 \mu\text{m}$) after *in vitro*
 369 digestion. Different letters in each evaluated parameter represent significant differences between the
 370 tested Pickering emulsions ($p < 0.05$; one-way ANOVA): ^{a-b} for bioaccessibility, ^{A-B} for stability, and ^{x-y} for
 371 effective bioavailability.

372

373 The low observed bioaccessibility for the tested PEs can be attributed to the high amount
 374 of free Ca^{2+} ions derived from the n-HAp particles disruption in the gastric phase. Ca^{2+}
 375 ions can form insoluble aggregates with anionic species, such as bile salts and free fatty
 376 acids, decreasing the mixed micelle's formation. Additionally, Ca^{2+} can also form

377 aggregates with PO_4^{2-} species (random calcium phosphates). These aggregates can entrap
378 the lipidic phase, hindering its digestion and, consequently, the micellar phase formation.
379 The CLSM images taken after the intestinal phase (**Figure 6**) support this hypothesis. In
380 fact, the insoluble aggregates (stained in red) and the lipidic phase (stained in green) are
381 superimposed, meaning that some lipidic phase remained entrapped inside these
382 structures. In addition, the insoluble aggregates can also entrap the mixed micelles
383 containing the vitamin E, fact in accordance with the observed high stability and low
384 bioaccessibility, as also reported by (Yang et al., 2015) in a work addressing vitamin E.
385 Zhou et al. (2020), which compared the effect of using PEs produced with nanochitin
386 particles with emulsions produced with Tween 80 on vitamin D_3 bioaccessibility, reported
387 a lower bioaccessibility for PEs. The authors justified these results by the precipitation of
388 the mixed micelles in the presence of the nanochitin together with the presence of the
389 non-digested vitamin D_3 lipid phase carrier. Additionally, Tan et al. (2020) examined the
390 impact of using chitosan on vitamin D_3 bioaccessibility with results showing that it
391 promoted severe droplet flocculation in the small intestine, reducing the amount of free
392 fatty acids and leading vitamin D_3 bioaccessibility decrease. This effect was justified by
393 chitosan ability to bound with vitamin-loaded mixed micelles promoting their
394 precipitation.



395

396 Figure 6: CLSM images Pickering emulsions (NET-low, NET-middle and NET-high) after intestinal
 397 phase.

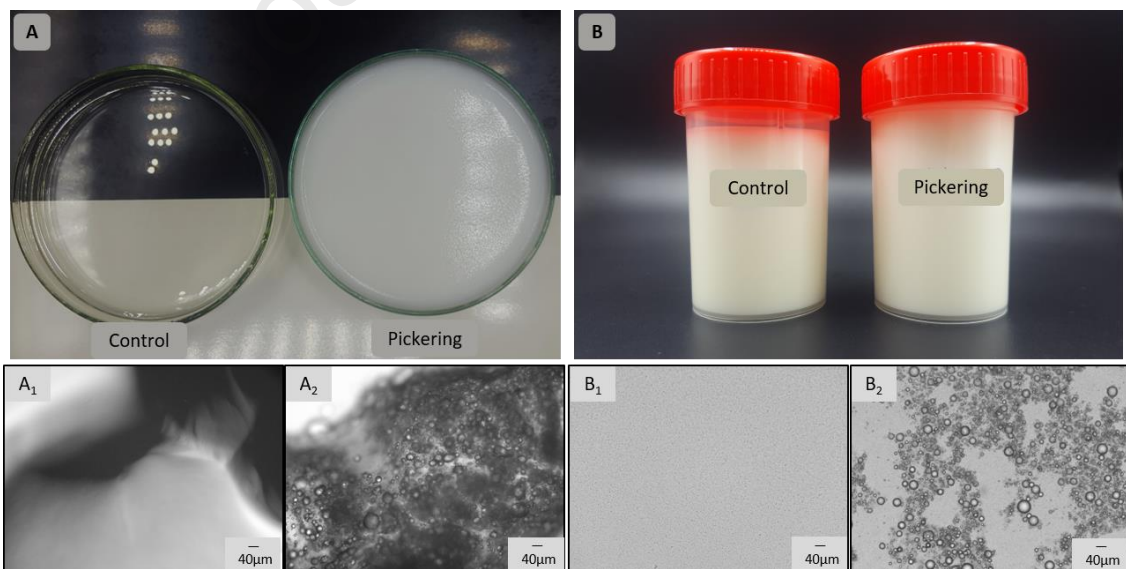
398

399 The NET-high sample presented a slightly, but significantly higher vitamin E
 400 bioaccessibility, comparatively with the other tested emulsions ($p < 0.05$). This can be
 401 associated to the observed droplet size for this emulsion after the gastric phase. Once the
 402 NET-high sample had a higher droplet size, the lipid digestion rate at the intestinal phase
 403 was, probably, slower than the ones of other emulsions, meaning that the formation of the
 404 mixed micelles delayed the Ca^{2+} ions binding to other ionic species. Therefore, the
 405 presence of Ca^{2+} ions showed to have a high impact on vitamin E bioaccessibility and
 406 stability. Moreover, the PE produced with the larger particle size (NET-high) lead to
 407 better results in terms of vitamin E bioaccessibility.

408 3.3 Vitamin E fortified foods

409 The PE presenting the best vitamin E bioaccessibility after digestion (NET-high) was
 410 incorporated in gelatine and milk to study the effect of the food matrix in this parameter.
 411 Gelatine is constituted only by proteins and milk comprises fat, proteins and

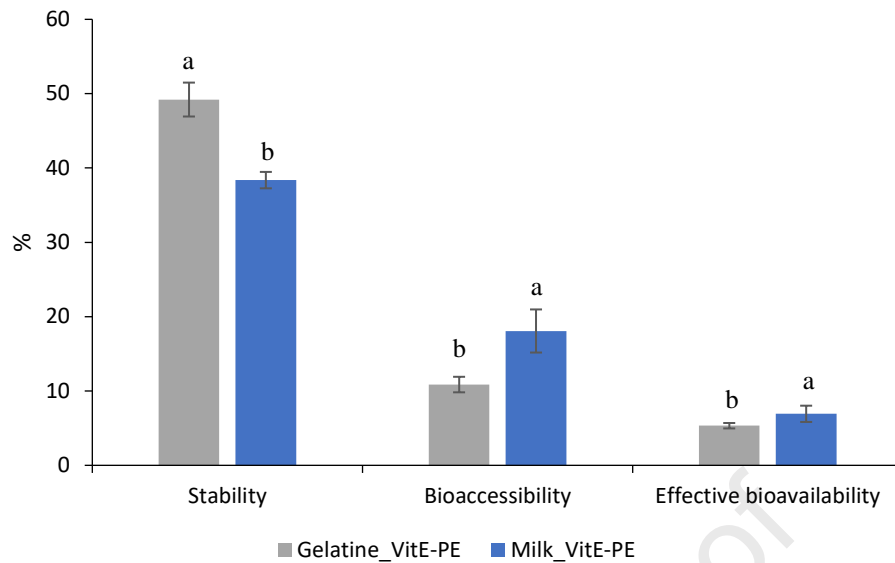
412 carbohydrates. Both foods are widely consumed. Inorganic solid particles are usually
 413 used in the food industry to modify properties such as viscosity, brightness, and whiteness
 414 (Weir, Westerhoff, Fabricius, Hristovski, & von Goetz, 2012; Zhou et al., 2021). In this
 415 work, the n-HAp solid particles were used as stabilizers in PEs for vitamin E carriers,
 416 thus contributing to the organoleptic properties and to add functional properties to foods.
 417 **Figure 7** shows the photos of the used food matrices, gelatine (**Figure 7-A**) and milk
 418 (**Figure 7-B**) without incorporation (control samples) and after the incorporation of the
 419 vitamin E-loaded PE (fortified foods). In gelatine, the emulsion addition changes the
 420 sample from transparent to white, effect clearly observed. Regarding milk, no significant
 421 macroscopic changes in terms of colour were observed. In **Figure 7-A1** and **A2**, and
 422 **Figure 7-B1** and **B2** the optical microscopy images of gelatine and milk (control sample
 423 and fortified food, respectively) are shown. It is possible to observe a clean and
 424 homogeneous image for the control food matrices, whereas for the fortified foods the
 425 presence of the PE is noticeable. To note that the Pickering droplets remained with their
 426 typical morphology and size after incorporation.



427

428 Figure 7: Photos of control samples and fortified foods: gelatine (A) and milk (B). Optical microscopy
 429 images for gelatine and milk controls, (A₁ and B₁, respectively), and fortified gelatine and milk (A₂ and
 430 B₂, respectively). Images were acquired at a magnification of 10x.

431 After emulsion incorporation, the fortified foods (fortified milk and fortified gelatine)
432 were digested to access vitamin E stability and bioaccessibility. To check for any food
433 matrix or PE materials effects, control samples (foods without incorporation, and foods
434 added with non-loaded PEs) were also *in vitro* digested to determine vitamin E presence.
435 **Figure 8** shows the stability, bioaccessibility and bioavailability of the vitamin E after
436 fortified gelatine and fortified milk digestion, the statistical analysis was done to compare
437 the fortified foods for each evaluated parameter. In general, the two fortified foods lead
438 to good vitamin E stability, with fortified gelatine (gelatine_VitE-PE) showing higher and
439 statistically different vitamin E stability, comparatively with fortified milk (milk_vitE-
440 PE), namely $49.2\pm 2.28\%$ and $38.4\pm 1.10\%$, respectively ($p<0.05$). Comparing the two
441 fortified foods, the milk_vitE-PE sample presented higher and statistically different
442 bioaccessibility, $18.1\pm 2.90\%$, in comparison with $10.9\pm 1.04\%$ for gelatine_VitE-PE
443 ($p<0.05$). In addition, milk_vitE-PE presented higher and statistically different
444 bioavailability than gelatine_VitE-PE ($6.93\pm 1.09\%$ and $5.33\pm 0.36\%$, respectively)
445 ($p<0.05$). To note that the control samples (foods without incorporation) presented no
446 vitamin E (data not shown). In the case of foods added with non-loaded PEs, only a very
447 residual vitamin E content, attributed to the sunflower oil, was detected (data not shown).
448 Thus, the quantified vitamin E after digestion of the fortified foods was related to the
449 incorporated vitamin E-loaded PEs.



450

451 Figure 8: Bioaccessibility, stability and adequate bioavailability of fortified food with vitamin E loaded
 452 Pickering emulsions (NET-high: $\sim 18 \mu\text{m}$) after *in vitro* digestion. Different letters represent significant
 453 differences between fortified food matrices in each parameter ($p < 0.05$; *t*-test): ^{a-b} for bioaccessibility, ^{A-B}
 454 for stability, and ^{x-y} for adequate bioavailability.

455

456 One important point to highlight is the fact that fortified foods lead to better vitamin E
 457 bioaccessibility and stability in comparison with the non-incorporated vitamin E-loaded
 458 PEs. Namely, for vitamin E-loaded PEs, the maximum achieved bioaccessibility and
 459 stability values were $3.29 \pm 0.57\%$ and $28.9 \pm 2.59\%$, respectively, for the sample NET-high,
 460 which is much lower than the values obtained with fortified milk ($18.1 \pm 2.90\%$ and
 461 $38.4 \pm 1.10\%$ for bioaccessibility and stability, respectively) and fortified gelatine
 462 ($10.9 \pm 1.04\%$ and $49.2 \pm 2.28\%$ for bioaccessibility and stability, respectively). The natural
 463 presence of macronutrients in the fortified foods led to a vitamin E bioaccessibility
 464 increase, possibly associated with their ability to displaced some n-HAp particles from
 465 the oil droplet's surface, facilitating lipid digestion, vitamin E release and solubilisation,
 466 and mixed micelles formation (Zhou et al., 2020). Furthermore, fortified milk presented
 467 a slightly higher bioaccessibility than gelatine, which can be related to fat presence in this
 468 food matrix, which can improve the micellar phase formation. This can be explained
 469 because the mixed micelles generated during the lipid digestion had more free-fatty acids

470 available for their formation. Therefore, if a higher number of mixed micelles can be
471 formed, more vitamin E can be incorporated leading to an increased bioaccessibility.
472 Another fact contributing positively to vitamin E bioaccessibility is the lower amount of
473 n-HAp particles presented in the fortified food. This leads to the formation of less Ca^{2+}
474 species, decreasing aggregates formation. Additionally, the incorporation of vitamin E-
475 loaded PE in gelatine and milk also lead to an increased vitamin E stability, which
476 indicates lower vitamin E loss during GI digestion.

477 Although considering different lipophilic vitamins, the results reported in the present
478 work for bioaccessibility agree with those published by Zhou et al. (2021). The plant-
479 based milk fortified with a vitamin D₃-loaded emulsion together with nanocellulose or
480 titanium dioxide particles showed a vitamin D₃ bioaccessibility around 20% (Zhou et al.,
481 2021).

482 **4 Conclusion**

483 The interest in using PEs as carriers of lipophilic vitamins, foreseeing their use in fortified
484 foods, is a topic gathering interest within the scientific community. This implies the
485 digestion study of both PEs and fortified foods to have a more complete image of the
486 parameters impacting vitamin bioaccessibility. In this study, n-HAp Pickering emulsions
487 are proposed as vitamin E carriers, and the impact of droplet size (7.53, 11.56 and
488 17.72 μm) in vitamin E stability, bioaccessibility and bioavailability was studied. For
489 that, emulsions with tailored droplet size were produced by NETmix, a static mixer
490 enabling continuous production at controlled emulsifying conditions.

491 In terms of digestion, the tested vitamin E-loaded PEs presented similar behaviour along
492 the GIT, with n-HAp particles being disrupted in gastric conditions with subsequent
493 formation of aggregates under intestinal environment. The droplet average size impacted
494 vitamin E bioaccessibility, with the NET-high sample, i.e., the sample with the higher

495 droplet size ($17.72\ \mu\text{m}$), leading to the higher vitamin E bioaccessibility results
496 ($3.29\pm 0.57\%$). The achieved low values were associated with the entrapment of the oil
497 phase containing vitamin E within the formed random calcium aggregates (intestinal
498 phase). When the vitamin E-loaded PE NET-high was incorporated in food matrices
499 (gelatine and milk), vitamin E bioaccessibility increased significantly ($10.87\pm 1.04\%$ for
500 gelatine and $18.07\pm 2.90\%$ for milk), putting in evidence the positive effect of the food
501 matrix in the bioaccessibility.

502 Overall, n-HAp Pickering emulsions offer advantages for vitamin E encapsulation
503 directed to fortified foods development, a process able to be extended to other lipophilic
504 vitamins, and to other Pickering stabilizers. The obtained results also pointed out the
505 interest proceed with further studies, namely to understand the effect of the food matrix
506 composition in the achieved bioaccessibility. Moreover, it also highlights the importance
507 of combining the study of PEs with their final applications to evaluate more accurately
508 the real potential of these innovative solutions.

509 **Acknowledgements**

510 This work was financially supported by Base Funding - UIDB/50020/2020 of the
511 Associate Laboratory LSRE-LCM - funded by national funds through FCT/MCTES
512 (PIDDAC), Base Funding - UIDB/00690/2020 of CIMO - funded by national funds
513 through FCT/MCTES (PIDDAC), and Base Funding - UIDB/04469/2020 of the CEB
514 funded by national funds through FCT. Andreia Ribeiro acknowledges her PhD
515 fellowship funded by Project NORTE-08-5369-FSE-000028, supported by N2020, under
516 PT2020, through ESF, and Raquel F. Gonçalves acknowledges the Foundation for
517 Science and Technology (FCT) for their fellowship (SFRH/BD/140182/2018). Authors
518 thank Fluidinova S.A. for providing samples of *nanoXIM-CarePaste* and Instituto de
519 Investigação e Inovação em Saúde (i3S) for the services provided with CLSM analysis.

520 **References**

- 521 AOCS. (2003). *Official methods and recommended practices of the American Oil Chemists*
522 *Society* (5th ed.).
- 523 Borel, P., Preveraud, D., & Desmarchelier, C. (2013). Bioavailability of vitamin E in humans: an
524 update. *Nutr Rev*, *71*(6), 319-331. doi: 10.1111/nure.12026
- 525 Brodkorb, A., Egger, L., Alminger, M., Alvito, P., Assunção, R., Ballance, S., . . . Recio, I. (2019).
526 INFOGEST static in vitro simulation of gastrointestinal food digestion. *Nature Protocols*,
527 *14*(4), 991-1014. doi: <https://doi.org/10.1038/s41596-018-0119-1>
- 528 Burton, G. W. (1994). Vitamin E: molecular and biological function. *Proc Nutr Soc*, *53*(2), 251-
529 262. doi: <https://doi.org/10.1079/pns19940030>
- 530 Epple, M. (2018). Review of potential health risks associated with nanoscopic calcium phosphate.
531 *Acta Biomaterialia*, *77*, 1-14. doi: <https://doi.org/10.1016/j.actbio.2018.07.036>
- 532 Hategekimana, J., Masamba, K. G., Ma, J., & Zhong, F. (2015). Encapsulation of vitamin E:
533 Effect of physicochemical properties of wall material on retention and stability.
534 *Carbohydrate Polymers*, *124*, 172-179. doi:
535 <https://doi.org/10.1016/j.carbpol.2015.01.060>
- 536 Hategekimana, J., & Zhong, F. (2015). Degradation of Vitamin E in Nanoemulsions during
537 Storage as Affected by Temperature, Light and Darkness. *International Journal of Food*
538 *Engineering*, *11*(2), 199–206. doi: <https://doi.org/10.1515/ijfe-2014-0256>
- 539 Katouzian, I., & Jafari, S. M. (2016). Nano-encapsulation as a promising approach for targeted
540 delivery and controlled release of vitamins. *Trends in Food Science & Technology*, *53*,
541 34-48. doi: <https://doi.org/10.1016/j.tifs.2016.05.002>
- 542 Lv, S., Zhang, Y., Tan, H., Zhang, R., & McClements, D. J. (2019). Vitamin E Encapsulation
543 within Oil-in-Water Emulsions: Impact of Emulsifier Type on Physicochemical Stability
544 and Bioaccessibility. *Journal of Agricultural and Food Chemistry*, *67*(5), 1521-1529. doi:
545 <https://doi.org/10.1021/acs.jafc.8b06347>
- 546 McClements, D. J. (2016). *Food emulsions: principles, practices, and techniques* (3rd ed.).
547 London: CRC Press.
- 548 Minekus, M., Alminger, M., Alvito, P., Ballance, S., Bohn, T., Bourlieu, C., . . . Brodkorb, A.
549 (2014). A standardised static in vitro digestion method suitable for food - an international
550 consensus. *Food Funct*, *5*(6), 1113-1124. doi: <https://doi.org/10.1039/c3fo60702j>
- 551 Mitbumrung, W., Suphantharika, M., McClements, D. J., & Winuprasith, T. (2019).
552 Encapsulation of Vitamin D3 in Pickering Emulsion Stabilized by Nanofibrillated
553 Mangosteen Cellulose: Effect of Environmental Stresses. *Journal of Food Science*,
554 *84*(11), 3213-3221. doi: 10.1111/1750-3841.14835
- 555 Mujica-Álvarez, J., Gil-Castell, O., Barra, P. A., Ribes-Greus, A., Bustos, R., Faccini, M., &
556 Matiacevich, S. (2020). Encapsulation of Vitamins A and E as Spray-Dried Additives for
557 the Feed Industry. *Molecules (Basel, Switzerland)*, *25*(6), 1357. doi:
558 <https://doi.org/10.3390/molecules25061357>
- 559 Niki, E., & Noguchi, N. (2020). Antioxidant action of vitamin E in vivo as assessed from its
560 reaction products with multiple biological oxidants. *Free Radical Research*, 1-12. doi:
561 <https://doi.org/10.1080/10715762.2020.1866181>
- 562 Ramis, J. M., Coelho, C. C., Córdoba, A., Quadros, P. A., & Monjo, M. (2018). Safety assessment
563 of nano-hydroxyapatite as an oral care ingredient according to the EU cosmetics
564 regulation. *Cosmetics*, *5*(3), 53-66. doi: <https://doi.org/10.3390/cosmetics5030053>

- 565 Ribeiro, A., Manrique, Y. A., Barreiro, F., Lopes, J. C. B., & Dias, M. M. (2021). Continuous
566 production of hydroxyapatite Pickering emulsions using a mesostructured reactor.
567 *Colloids and Surfaces A: Physicochemical and Engineering Aspects*, 616, 126365-
568 126376. doi: <https://doi.org/10.1016/j.colsurfa.2021.126365>
- 569 Tan, Y., Li, R., Liu, C., Mundo, J. M., Zhou, H., Liu, J., & McClements, D. J. (2020). Chitosan
570 reduces vitamin D bioaccessibility in food emulsions by binding to mixed micelles. *Food
571 & Function*, 11, 187-199. doi: <https://doi.org/10.1039/C9FO02164G>
- 572 Weir, A., Westerhoff, P., Fabricius, L., Hristovski, K., & von Goetz, N. (2012). Titanium Dioxide
573 Nanoparticles in Food and Personal Care Products. *Environmental Science &
574 Technology*, 46(4), 2242-2250. doi: <https://doi.org/10.1021/es204168d>
- 575 Winuprasith, T., Khomein, P., Mitbumrung, W., Suphantharika, M., Nitithamyong, A., &
576 McClements, D. J. (2018). Encapsulation of vitamin D3 in pickering emulsions stabilized
577 by nanofibrillated mangosteen cellulose: Impact on in vitro digestion and
578 bioaccessibility. *Food Hydrocolloids*, 83, 153-164. doi:
579 <https://doi.org/10.1016/j.foodhyd.2018.04.047>
- 580 Yang, Y., Decker, E. A., Xiao, H., & McClements, D. J. (2015). Enhancing vitamin E
581 bioaccessibility: factors impacting solubilization and hydrolysis of α -tocopherol acetate
582 encapsulated in emulsion-based delivery systems. *Food Funct*, 6(1), 84-97. doi:
583 <https://doi.org/10.1039/c4fo00725e>
- 584 Yang, Y., & McClements, D. J. (2013). Vitamin E bioaccessibility: Influence of carrier oil type
585 on digestion and release of emulsified α -tocopherol acetate. *Food Chemistry*, 141(1), 473-
586 481. doi: <https://doi.org/10.1016/j.foodchem.2013.03.033>
- 587 Zhou, H., Liu, J., Dai, T., Muriel Mundo, J. L., Tan, Y., Bai, L., & McClements, D. J. (2021). The
588 gastrointestinal fate of inorganic and organic nanoparticles in vitamin D-fortified plant-
589 based milks. *Food Hydrocolloids*, 112, 106310. doi:
590 <https://doi.org/10.1016/j.foodhyd.2020.106310>
- 591 Zhou, H., Tan, Y., Lv, S., Liu, J., Muriel Mundo, J. L., Bai, L., . . . McClements, D. J. (2020).
592 Nanochitin-stabilized pickering emulsions: Influence of nanochitin on lipid digestibility
593 and vitamin bioaccessibility. *Food Hydrocolloids*, 106, 105878. doi:
594 <https://doi.org/10.1016/j.foodhyd.2020.105878>
- 595

Highlights

NETmix was successfully used to produce vitamin E-loaded Pickering emulsions.

Hydroxyapatite disrupts in the stomach solubilizing in the aqueous medium.

The formation of calcium aggregates in the intestine hinder vitamin E bioaccessibility.

Higher droplet size Pickering emulsions enhanced vitamin E bioaccessibility.

Incorporation of Pickering emulsions in foods improved vitamin E bioaccessibility.

Declaration of interests

The authors declare that they have no known competing financial interests or personal relationships that could have appeared to influence the work reported in this paper.

The authors declare the following financial interests/personal relationships which may be considered as potential competing interests:

Journal Pre-proof